

DETECTION OF LANE DEPARTURE ON HIGH-SPEED ROADS

David Hanwell and Majid Mirmehdi

University of Bristol, Bristol, U.K.

Keywords: Lane departure, Lane tracking, Vanishing point.

Abstract: We present a system for detecting and tracking the lanes of high-speed roads, in order to warn the driver of accidental lane departures. The proposed method introduces a novel variant of the classic Hough transform, better equipped to detect and locate linear road markings with a common vanishing point. This is combined with a simple model of the lane and an Extended Kalman Filter to make detection and tracking more robust. This allows detection of lane changes, resistant to visual interference by traffic and irrelevant road markings.

1 INTRODUCTION

Studies have shown that many accidents are caused by drivers falling asleep (Horne and Reyner, 1995), especially during long journeys on high speed roads. In such cases, mortality rates tend to be higher as the driver is not sufficiently alert to brake or steer to avoid obstacles (NCSDR/NHTSA Expert Panel on Driver Fatigue and Sleepiness, 1998). Even when wide awake, a driver's inattentiveness can cause accidents, e.g. due to failure to check for other vehicles in blind spots when changing lanes. Recently, some vehicle manufacturers have begun to incorporate cameras into their cars, for example to provide a more favorable rear-view when reversing. Using these to produce a lane departure warning system (LDWS) could help reduce both the number and severity of accidents (Rimini-Doering et al., 2005).

For its use to become widespread, a LDWS should be as cheap and simple to install as possible, requiring minimal additional hardware. Much of the previous work in lane detection and tracking looks at the more involved problem of autonomous driving, requiring extra hardware for a more elaborate approach to lane departure detection, e.g. many use multiple cameras (Loose and Franke, 2010; Lipski et al., 2008).

Accidental lane departures are most common, and most dangerous, on high speed roads. Such roads tend to have low curvature, appearing almost straight, especially from our camera's viewpoint, mounted on the front bumper significantly below driver eye view (see Fig. 5(a) for an example). We exploit this fact to simplify both the detection and modelling of lane markings and present a system which uses only a single camera, and requires no more computational power

than provided by a standard PC. The data is obtained from an experimental vehicle by Jaguar Land Rover.

In order for a LDWS to be effective, it must be resilient to visual clutter. Specifically, it should (a) detect only those image features which correspond to road markings, i.e. ignore road barriers, or other traffic, (b) ignore irrelevant road markings, i.e. writing on road surfaces or road markings not parallel to the vehicle's lane, and (c) be able to detect and track not only those markings delimiting the vehicle's immediate lane, but also adjacent lanes to allow tracking to be uninterrupted during, and after, a lane change.

For each of the above criteria, one can find examples of its use in previous work, but no single piece of work incorporates all three into a single camera system. In the case of the 1st for example, (Wu et al., 2009) describes a system which exploited the contrast of road markings against their background. They used transitions in image intensity, with a statistical search algorithm, to find road markings. Most others however, simply sought strong edge lines (McDonald, 2001; Voisin et al., 2005; Jung and Kelber, 2005). While road markings do tend to have strong edges, not all strong edges correspond to road markings, and so it can be prone to interference, e.g. from other traffic.

Approaches to the 2nd criteria usually involve taking into account the expected position and orientation of road markings. For example in (McDonald, 2001), the vanishing point (VP) of the road markings was presumed to lie in a fixed rectangular region of the image. A Hough transform (HT) was applied to this rectangle, and the accumulator binarised, giving a map of the points in the Hough space that represent lines which pass through the rectangular region. This was then used as a mask for the accumulator during

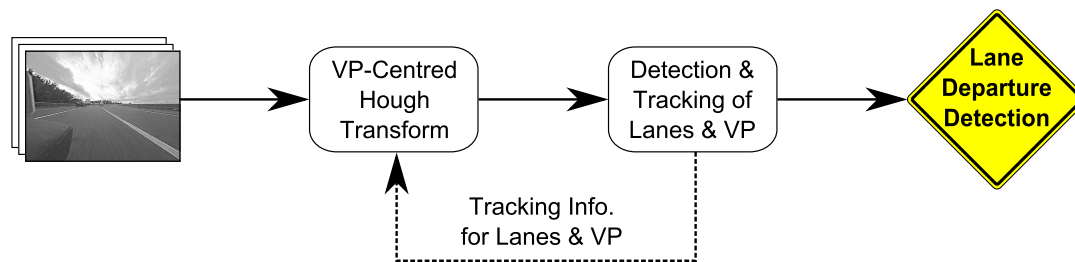


Figure 1: An overview of the system.

the detection of lane edge lines, thus filtering out any detected edges unlikely to belong to road lane markings. In (Jung and Kelber, 2005), a histogram of edge pixel directions was used in a weighted HT to extract the edge lines in the most common directions. The authors state this worked well but could be prone to interference from other ‘significant structures’ in the image, or from vehicles close in front.

Of the three criteria, the 3rd is perhaps the least common, with most previous work concentrating on tracking only two (Voisin et al., 2005; Wu et al., 2009; Jung and Kelber, 2005) or three (McDonald, 2001; D’Cruz and Jia Zou, 2007) road markings. One notable exception is (Ieng et al., 2005), in which arbitrarily many road markings were simultaneously tracked, each with a separate Kalman filter (KF). However, the width of each lane was not taken into account, and multiple cameras were required.

While many of the above show good results in lane tracking, none take into account all three criteria, and so are not ideally suited to LDWS. We propose a simple LDWS method that detects and tracks the lanes of high speed roads, and addresses all three criteria. We demonstrate insensitivity to both nearby traffic and irrelevant road markings. Our method begins with a novel variant of the classic HT which is better equipped to detect and locate linear road markings with a common VP (Section 4). It uses knowledge of the VP location to detect only those road markings parallel to the lane. Also, it takes advantage of the distinctive appearance of linear road markings, to distinguish them from other lines parallel to the lane, e.g. edges of vehicles or road barriers. This is combined with an Extended Kalman Filter (EKF) to detect (Section 4.1) and track (Section 4.2) arbitrarily many road markings which are then used to estimate the VP location by an MSE minimisation method (Section 5). The VP is tracked between frames using a KF, and used by the HT to allow it to ignore edge lines not parallel to the lane. Its y-coordinate is used to define the ROI, allowing us to ignore objects above the horizon. A system overview is shown in Fig. 1. Section 6 presents our results, and demonstrates the robustness of our system on both straight and curved sections

of high-speed roads, and its robustness to occlusions. The paper is concluded in Section 7.

2 CAMERA-VEHICLE SET-UP

Footage was taken using a colour video camera mounted on the front bumper of the vehicle, 58cm above the ground. The camera has a horizontal field of view of 157° , resulting in severe fish-eye distortion, making a correction necessary. The result is an anti-aliased, greyscale image, conforming to a rectilinear projection. Mounted so low, the camera gives a different view from that usually seen by a driver (see Fig. 5(a)). It points forward, so that the horizon is approximately halfway up the image, allowing us to ignore the upper part of the image once the VP is found. Also, because the camera is mounted so low down, more distant road is contained within a much smaller area of image than nearer road, making more distant road markings difficult to distinguish. However, the low camera position causes road markings in the image to be less affected by the road’s curvature, allowing the system to function well even on curves. The choice of lens and camera position was not ours, but that of the vehicle manufacturer. The camera is one of six fitted to this model of vehicle, serving a variety of purposes including reversing and parking aids.

3 THE ROAD MARKING MODEL

In order to determine whether the vehicle has crossed a lane boundary, we must model the relationship between lines in the ground plane, and their corresponding lines in the image. This relationship is used to facilitate the detection and tracking of road markings. We use a standard pinhole camera model, with viewer axes X , Y , and Z , whose origin is the focal point. Our image plane has axes x and y , which lie parallel to the X and Y axes respectively.

We define a coordinate system in the ground plane, with axes u and v , and origin at $(0, h, 0)$ in

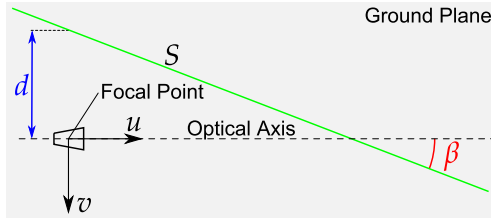


Figure 2: A top-down view of the parametrization of lines in the ground plane.

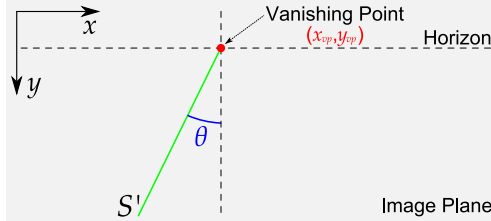


Figure 3: The parametrization of lines in the image plane, relative to the VP.

the viewer coordinate system, where h is the camera height above the ground. The v axis is parallel to the X and x axes, but the u axis is not necessarily parallel to the Z axis, due to the tilt, α , of the camera relative to the ground plane.

Now consider a straight line, S in the ground plane, such as a road marking's edge line, and assume that the VP of S in the image has already been determined to be at (x_{vp}, y_{vp}) (Section 5). The line S is parametrised by (d, β) , where d is its distance from the uv -axes origin along the v axis, and β is the angle at which it meets the u axis (Fig. 2). Hence, it is defined by $v = u \tan \beta - d$. The corresponding line in the image plane, S' (Fig. 3) is then:

$$y - y_{vp} = \frac{h}{d}(x - x_{vp}). \quad (1)$$

The line has slope h/d , hence a line in the ground plane parametrised by (d, β) will lie in the image plane at θ , i.e.

$$\theta = \frac{\pi}{2} + \tan^{-1} \left(\frac{h}{d} \right). \quad (2)$$

Thus, the lateral position, d , of a detected edge line in the ground plane relative to the camera, depends only upon θ , the angle at which it was detected, and so is invariant to translation. Crucially, this means that as long as we know the road markings' collective VP, we can describe the location of each using only one value, θ . This has two implications: firstly, it means we can separate the tracking of the VP and the road markings into two independent tasks, and secondly, it means that to track a road marking, we need only store its angle between frames.

In determining a white lane marking, we are interested in finding the pair of edge lines demarcating it. Suppose θ_1 and θ_2 are the angles of two edge lines in the image. We wish to determine the relationship between these two angles, and the perpendicular distance w , between the corresponding lines in the ground plane. Using (2) we can derive,

$$\theta_1 = g(\theta_2, w) = \tan^{-1} \left(\frac{w}{h} - \tan(-\theta_2) \right). \quad (3)$$

Hence, if we detect two road markings, we can determine the distance between them, and having detected one edge line of a road marking we can estimate the range of angles in which the other will lie.

4 NOVEL VARIANT OF THE HT

We begin by applying both horizontal and vertical Scharr filters (Jähne et al., 1999) to the greyscale input frame, to produce two gradient maps. Only those pixels whose gradient magnitude is above a (liberally selected) threshold go on to be represented in the Hough accumulator. When transforming an edge-pixel to the accumulator, instead of making an entry for every value of θ , we instead use only a narrow range, 2° each side of the edge-pixel's angle. This is intended to increase the speed at which the HT can be performed, and to increase accuracy by reducing the likelihood of erroneous maxima in the accumulator. An edge pixel's additions to the accumulator are *weighted* in proportion to its gradient. This results in shorter, more well defined edge lines being favoured over longer, more weakly defined ones. A similar modification was made in (Jung and Kelber, 2005) for the same reason.

Parallel road markings have a common VP in the image. We distinguish between those edge lines which pass through or close to this VP, and those which do not by first estimating the location of the VP, and then performing a translation of image coordinates, moving the origin to this estimated VP. We are then able to exploit the polar coordinate system inherent to the HT, by restricting the distance dimension, ρ , of the accumulator to a narrower range, and thus omit the parametrizations of lines which pass too far from the VP. This amounts to only considering lines which pass through a small circular region centred at the VP (Fig. 4). By tracking the VP, we allow this efficiency to continue for subsequent frames. This detection and tracking is expounded on in Section 5.

This contrasts with the method of (McDonald, 2001) in which the VP is not explicitly detected, but presumed to lie in a fixed rectangular region of the image. A mask for the Hough accumulator specifies

which parametrisations correspond to lines that pass through this rectangle. A possible shortcoming of this approach is that should the VP move out of the rectangle, none of the lane markings would be detected. In order to move or resize the detection region, a new mask would have to be created. Our method allows the image region through which lane edge lines must pass to be moved and resized as necessary, with no increase in computation, with its radius, ϕ , based on the covariance matrix of the VP KF (see Fig. 4). Furthermore, our method uses a smaller accumulator in which maxima can be found more quickly.

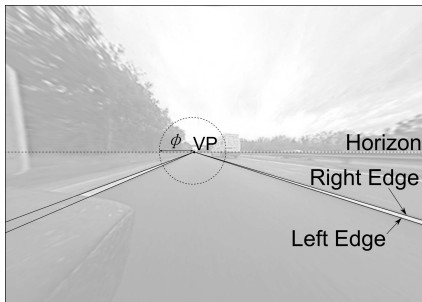


Figure 4: The circle of detection, and left and right edges.

Road markings are, by design, among the brightest objects on the road and have definite edges along the transition from bright white paint to darker grey road material. Since they are of constant width, they have two parallel edge lines of opposite gradient direction. We exploit both the sharpness of these gradients, and the fact that they occur in converse pairs, to distinguish them from other objects parallel to the lane, such as barriers and nearby vehicles.

Our accumulator is a 2D array, $A(\rho, \theta)$, where ρ specifies the perpendicular distance from a line to the origin, and θ is the angle of the line. We refer to edge pixels at which the image intensity increases in the anti-clockwise direction about the VP, as the *left edge* line of a road marking, and similarly, edge points at which the image intensity increases in the clockwise direction, as *right edge* line (Fig. 4). Each element of the 2D accumulator stores two values, l and r , corresponding to left and right edges respectively, i.e. $A(\rho, \theta) = (l, r)$.

Hence, the accumulator has two channels, a left channel and a right channel. When performing the HT, a pixel's gradient direction is used to determine which edge type it lies upon, and *its addition to the accumulator is then made to the corresponding channel*. This means each occurrence of a lane marking is characterised in the accumulator by a pair of relatively high values, not more than a certain distance apart, with one being in each channel.

To facilitate the identification of pairs of maxima

in the accumulator, the largest value is taken from each column of each channel of the accumulator and recorded along with the value of ρ at which it occurred, i.e. we obtain for each of the (l, r) channels in A , a 1D array of values, resulting in two arrays, $L(\theta)$ and $R(\theta)$, which we refer to as the left maximum array and the right maximum array respectively,

$$L(\theta) = (\hat{\rho}_\theta^l, \hat{l}_\theta), \quad R(\theta) = (\hat{\rho}_\theta^r, \hat{r}_\theta) \quad (4)$$

with,

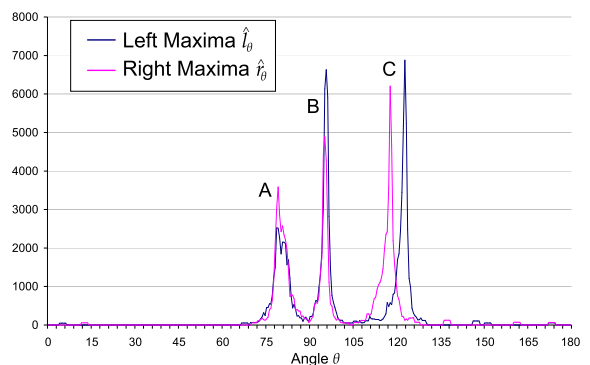
$$\hat{\rho}_\theta^l = \operatorname{argmax}_\rho (A^l(\rho, \theta)) \quad (5)$$

$$\hat{l}_\theta = \max_\rho (A^l(\rho, \theta)) \quad (6)$$

where A^l and A^r are the left and right channels of A respectively, and $\hat{\rho}_\theta^r$ and \hat{r}_θ are defined similarly. An example of a typical frame and a graph showing the contents of the maximum arrays resulting from our HT are shown in Fig. 5. The graph clearly shows three pairs of peaks, each representing one of the three road markings visible in the frame.



(a) A typical frame.



(b) A plot of the two maximum arrays derived from the Hough accumulator for the frame above.

Figure 5: Labels A, B, C mark the correspondence of the peaks in maxima arrays \hat{l}_θ and \hat{r}_θ to lane markings.

This reduction in dimension greatly simplifies lane marking detection, as we later describe. It makes

the assumption however, that for each θ -value, there will be at most one relevant maximum in each accumulator channel. This is equivalent to the assumption that no two relevant edge lines will be parallel in the image. We consider this to be a credible assumption for two reasons. Firstly, most linear objects in the road environment are parallel to the road, and hence share the same VP in the image as the road lane. This implies that their edge lines are not parallel in the image. Secondly, to be detected, edge lines must pass through a relatively small circle around the VP. If a detected edge line does have a parallel elsewhere in the image, it is unlikely that it will be detected.

To summarise, there are four key differences between our method and the classical HT method: (a) edge direction is taken into account when applying the transform to a pixel, (b) the values added to the accumulator are proportional to gradient magnitudes, (c) we move the image origin to the VP, so that accumulator maxima corresponding to relevant edges lie near $\rho = 0$, and (d) we use two accumulator channels for left and right edges.

4.1 Road Marking Detection

Once the maximum arrays for a frame have been computed, the average value is calculated over both arrays. This gives a measure of the overall edge strength in the frame, and is used to automatically set appropriate thresholds for road marking detection. This is intended to allow the system to quickly adapt to changing weather and light levels.

To simplify the process of detecting pairs of significant local maxima in the two maximum arrays, we ‘thin’ each array by suppressing secondary maxima. For each value of θ , we imagine a line at that angle. We use (3) to calculate what range of angles is likely to represent lines in the ground plane which lie within a small lateral distance w of that line. In the maximum arrays, we keep only the largest value in the range, and set the rest to zero. More formally, we replace each \hat{l}_θ by $f^l(\theta)$, where,

$$f^l(\theta) = \begin{cases} \hat{l}_\theta & \text{if } \hat{l}_\theta = \max_{\theta' \in G(\theta, w)} \hat{l}_{\theta'} \\ 0 & \text{otherwise} \end{cases} \quad (7)$$

where $G(\theta, w) = [g(\theta, -w), g(\theta, w)]$ with $g(\theta, w)$ as in (3). Values of \hat{r}_θ are treated similarly. The result is a sparse set of peaks, corresponding to lines that meet at the VP and we expect to be lane markings; for an example see Fig. 6.

As shown in Section 3, we can define each line parallel to the lane, by a single value, θ . We describe each road marking by the angle of its central

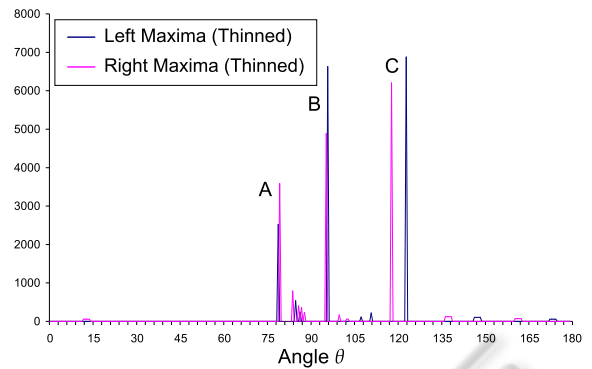


Figure 6: The data shown in Fig. 5(b) after ‘thinning’.

line, by averaging the angles of its two edge lines. Given this angle, and a maximal thickness of a linear road marking w , we use (3) to determine the appropriate range of θ to search in the maximum arrays. We determine w empirically to be approximately 32cm. To increase performance, the ranges of θ values are calculated off-line and stored in an array. We require peaks to be larger than a certain threshold, which is proportional to the automatic edge strength measure described above. We also impose other criteria, such as a maximal ratio between the peaks’ values, and a maximal difference between their corresponding ρ -values. Once a road marking is detected, its central angle is used to track it in the next frame.

Due to the lens and camera position employed in our system, road markings close to the vehicle take up a large proportion of the frame, and appear almost straight even on curved roads. For this reason, our method is appropriate even for roads of some curvature, and is especially useful for a LDWS since nearer road markings give the best indication of the vehicle’s current position relative to the lane.

4.2 Tracking of Road Markings

To track road markings, we use an EKF (see the model used in Fig. 7) which is able to track either one or two road markings. The approach used is to directly track those road markings which are of immediate concern, i.e. the ones which delimit the vehicle’s current lane. Then, the motion of the tracked markings is used to predict the locations of the road markings which are not tracked based on the assumption that all relevant road markings are parallel, and thus share the same lateral velocity relative to the camera. This is particularly useful in maintaining the tracking of dashed or occluded road markings

From (2) we can determine the position of a road marking in the ground plane to be,

$$\lambda = \tan(-\theta), \quad (8)$$

where θ is the angle of the line in the image plane, and λ is the lateral offset from the camera in units of h . There are three quantities which comprise the observation of the lane. The first two are the angles in the image plane at which each of the left and right lane boundary markings were detected, θ_l and θ_r , respectively. The third is the lateral velocity, v , which is measured using the changes in road markings' positions between frames. We calculate their lateral position on the ground plane, determine the movement of each, and take the mean. Lane width ψ is calculated as the difference in the lateral positions of the two road markings delimiting the lane.

If one of the two lane boundary markings is not detected in a frame, its position is inferred using the position of the other, and the model's current estimate of the lane width, ψ . Should neither lane boundary marking be detected, the model's prediction is used as the next model state, and the model state's covariance updated accordingly, bypassing the weighting and update stages. This continues until either one or both of the lane delimiting markings is explicitly detected, or until one of them has been absent for a sufficient number of frames that it is deemed no longer to exist. Similarly, if no estimate of v can be made, it is assumed to remain constant.

4.3 Management of Road Markings

For each tracked road marking, we store details such as its age (number of frames since first detection) and its recent absences (number of frames since last detected), which are used to decide whether or not it is a lane boundary. This increases robustness against mis-detections, e.g. by requiring that a road marking be detected in 4 consecutive frames before it is considered real. It also allows dashed and occluded road markings to be maintained in the list despite not being detected for several frames at a time, while at the same time not allowing such transient features as writing on the road surface to be mistaken for lane delimiters.

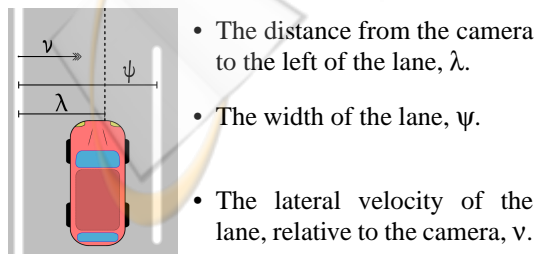


Figure 7: The model used in the EKF.

Given (8), we can calculate the lateral distance of a road marking from the camera using its angle in the

image. We can hence determine whether the vehicle is on top of, or close to, each road marking. This allows us to deduce whether the driver is in danger of making an accidental lane departure. We require that the vehicle be within 15cm of a lane boundary, or within 30cm and moving towards it, in order to trigger an alarm. These limits are easily adjustable to suit.

Should the vehicle approach a lane boundary quickly, this warning will occur very soon before the vehicle actually crosses the boundary. In order to warn the driver earlier, we use a third criterion which combines the distance from the lane boundary with the lateral velocity of the vehicle relative to it. In (Godthelp et al., 1984) the distance of a lane boundary from the vehicle is divided by the lateral velocity, to give a time-to-lane-crossing (TLC) value. We use the same method, and trigger an alarm whenever this TLC value falls below 25 frames. If employed on an actual vehicle, this alarm could be suppressed when the corresponding direction indicator is activated, thus detecting only *accidental* lane departures.

5 LOCATING & TRACKING THE VP

In (Cantoni et al., 2001) a method of estimating the VP in an image was proposed that involved a MSE minimization method to the contents of the Hough accumulator. We apply the same process but only to the parameters of detected road markings. This means fewer points must be processed, and, should the image contain multiple VPs, we can be more certain that we have identified the correct one.

Given N lines, parametrised by (ρ_i, θ_i) for $i = 1, \dots, N$, we estimate their VP $\hat{x}_{vp}, \hat{y}_{vp}$ as:

$$\hat{x}_{vp} = \frac{AE - CD}{AB - C^2}, \quad \hat{y}_{vp} = \frac{BD - CE}{AB - C^2}, \quad (9)$$

where,

$$A = \sum_{i=1}^N \sin^2 \theta_i, \quad B = \sum_{i=1}^N \cos^2 \theta_i, \quad C = \sum_{i=1}^N \cos \theta_i \sin \theta_i, \\ D = \sum_{i=1}^N \rho_i \sin \theta_i, \quad \text{and} \quad E = \sum_{i=1}^N \rho_i \cos \theta_i.$$

In order for a road marking's position to contribute to the estimate of VP location in a frame, it must have been detected in that frame and be old enough to be considered a genuine road marking (see Section 4.3). Lookup tables are used to increase performance.

To track the VP, a simple KF is used, with a constant position model consisting only of the VP's coordinates in the image. Though this is an almost trivial instance of a KF, it has an important advantage

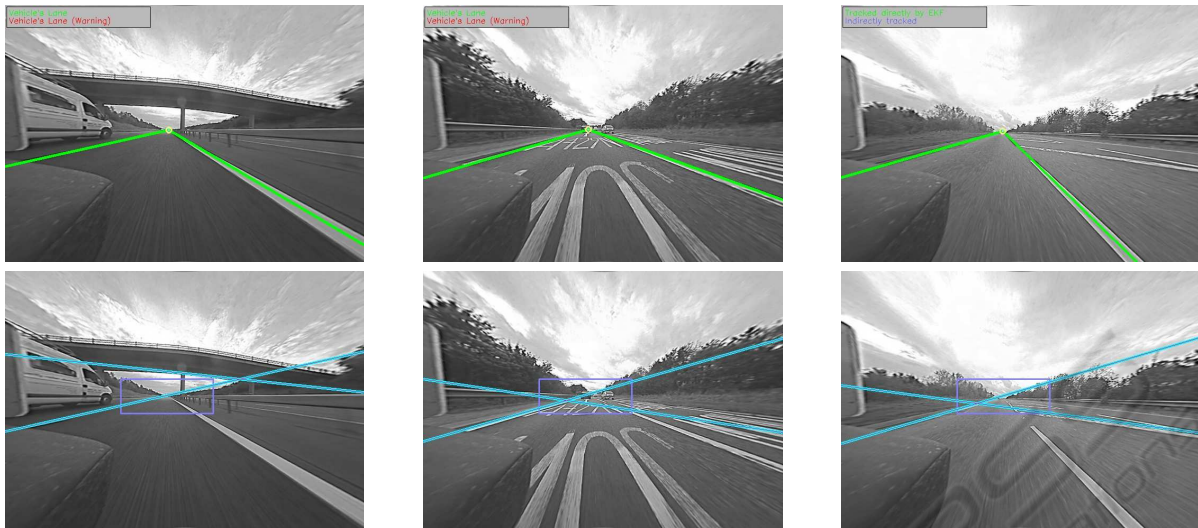


Figure 8: Our system (top) tracking lanes in the face of clutter, compared to McDonald (bottom).

over simpler methods such as exponential averaging. There may be frames in which insufficient road markings are found to give a reliable estimate of VP location. In such cases we simply use the model's prediction of VP location (i.e. that it remains where it is), but increase the model's covariance. When the VP's location can again be observed, the model will have higher variance, and so more weight will be given to the observation, resulting in the VP returning more quickly to its true coordinates. Quantitative experiments confirm that VP tracking accuracy is much improved by the KF (Section 6).

As the location of the VP is used in the detection of road markings, and the locations of road markings are used to determine the VP, the system requires an initial bootstrapping phase. This is achieved by initially setting the VP to be in the centre of the frame and using a large radius of detection in the HT. As road markings are detected, the covariance of the VP KF decreases, and the radius of detection with it. In our experiments, the VP KF typically takes around 1s to converge to the correct location.

6 RESULTS

We present our results, comparing against those of (McDonald, 2001), which is the closest work to ours in methodology. Though there are currently several commercially available LDWSs, we are unable to provide comparison with them as details of their methodology remain undisclosed. These include Mobileye's lane departure warning application (Mobileye[®] N.V., 2010), which is integrated into sev-

eral manufacturers' vehicles.

We also show examples of lanes being tracked despite transient occlusions. In our approach, we estimate the VP and do not process pixels above the horizon. McDonald's method does not locate the horizon or VP, so in order to make the comparison fair when applying McDonald's method to our data, we measured the ratio of image area above and below the horizon in the examples shown in (McDonald, 2001), and removed a portion of the frame in our data, to achieve a similar ratio. In the examples, for McDonald's method, the rectangle through which lines must pass in order to be detected is shown in lilac.

Fig. 9 shows two examples of lane change detection by the proposed method - in the left figure the vehicle is crossing to the left and in the right it is about to cross the lane to its right. Road markings being crossed are shown in red.

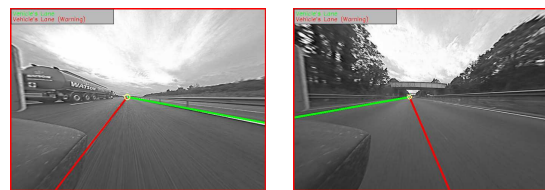


Figure 9: Examples of lane changes being detected.

Fig. 8 demonstrates key advantages of the proposed method. Firstly, strong edges not belonging to road markings are not detected. McDonald's method (McDonald, 2001) is confused by strong edges, e.g. in the 1st column of Fig. 8, the edge between the underside of a bridge and the sky, is detected as a road marking. Because (McDonald, 2001) only tracks two

road markings, when some other object is mistaken for a road marking, a real road marking goes undetected. Our proposed method does not detect strong non-lane edges for two reasons. Firstly, estimating the VP allows everything above the horizon to be ignored, and so other vehicles or objects on the roadside have much less influence. Secondly, instead of simply detecting edge lines, our method requires them to be correctly paired, and so edges which do not correspond to road markings are not detected.

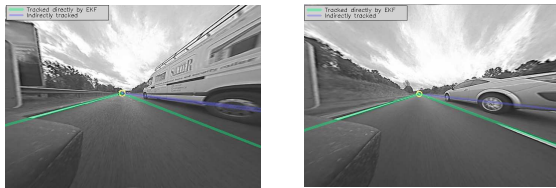


Figure 10: Lane markings being tracked through occlusion.

In general, our method shows high detection accuracy and good resistance to visual clutter. As Fig. 8 demonstrates, McDonald's method copes less well with such interference. In these respects, we fulfil the first two of the criteria outlined in Section 1. Since we track multiple road markings, our method also satisfies the third criteria. Fig. 10 shows tracking of lane markings through occlusion by nearby vehicles.

We performed a quantitative assessment of our VP tracking by first manually determining the VP in 200 consecutive frames. Then we measured the distance between the proposed method's VP location and the ground truth to have a mean of 2.0 pixels with a variance of 2.7. With the KF turned off, the mean was 4.4 pixels with a variance of 15.7.

Using a single thread on an Intel Core i5-660 CPU at 3.33 GHz, our system can achieve an average performance of 64 fps. The proposed method involves a few parameters, for example, how long a road marking is tracked for before it is considered to be a lane boundary, and how long one goes undetected before it is dropped by the system. The values for all our parameters have been empirically determined and remained constant in all the experiments.

7 CONCLUSIONS

We described a novel variant of the HT for the detection and tracking of linear road markings, with several novel refinements to the classical HT method, including the use of two accumulators and the translation of image coordinates to put their origin at the VP to facilitate more efficient analysis, such as ignoring road markings which are not parallel to the lane. The VP

is also detected and tracked, and feeds back into the HT process for subsequent frames. The method exhibits real-time performance with spare capacity for additional tasks.

ACKNOWLEDGEMENTS

The authors would like to thank Jaguar Land Rover for their support and supply of videos.

REFERENCES

- Cantoni, V., Lombardi, L., Porta, M., and Sicard, N. (2001). Vanishing point detection: Representation analysis and new approaches. In *Proc. of ICIAAP*.
- D'Cruz, C. and Jia Zou, J. (2007). Lane detection for driver assistance and intelligent vehicle applications. In *ISCIT 2007*, pp. 1291–1296.
- Godthelp, H., Milgram, P., and Blaauw, G. (1984). The development of a time-related measure to describe driving strategy. *Human Factors: Journal of HFES*.
- Horne, J. A. and Reyner, L. A. (1995). Sleep related vehicle accidents. *BMJ*, 310(6979):565–567.
- Jeng, S.-S., Vrignon, J., Gruyer, D., and Aubert, D. (2005). A new multi-lanes detection using multi-camera for robust vehicle location. In *Proc. IEEE IV*, pp. 700–705.
- Jähne, B., Scharr, H., and Körkel, S. (1999). *Handbook of Computer Vision and Applications*, pp. 125–152.
- Jung, C. R. and Kelber, C. R. (2005). Lane following and lane departure using a linear-parabolic model. *Image and Vision Computing*, 23(13):1192–1202.
- Lipski, C., Scholz, B., Berger, K., Linz, C., Stich, T., and Magnor, M. (2008). A fast & robust approach to lane marking detection & lane tracking. In *SSIAI*, pp. 57–60.
- Loose, H. and Franke, U. (2010). B-spline-based road model for 3d lane recognition. In *Proc 13th Intelligent Transportation Systems*, pp. 91–98.
- McDonald, J. (2001). Application of the HT to lane detection & following on high speed roads. In *ISSC*.
- Mobileye® N.V. (2010). Lane Departure Warning. <http://www.mobileye.com>.
- NCSDR/NHTSA Expert Panel on Driver Fatigue and Sleepiness (1998). *Drowsy driving and automobile crashes, Report No. DOT HS 808 707*.
- Rimini-Doering, M., Altmueller, T., Ladstaetter, U., and Rossmeier, M. (2005). Effects of lane departure warning on drowsy drivers performance and state in a simulator. In *3rd Int. Driving Symp. on Human Factors in Driver Assessment, Training, & Vehicle Design*, pp. 88–95.
- Voisin, V., Avila, M., Emile, B., Begot, S., and Bardet, J.-C. (2005). Road markings detection and tracking using Hough transform and Kalman filter. In *Advanced Concepts for Intelligent Vision Systems*, pp. 76–83.
- Wu, B.-F., Lin, C.-T., and Chen, Y.-L. (2009). Dynamic calibration and occlusion handling algorithms for lane tracking. In *IEEE TIE*, vol. 56, pp. 1757–1773.